Methodology of Power Distribution System Design for Hybrid Short Sea Shipping

Lana Andrey, Pinomaa Antti, Peltoniemi Pasi, Lahtinen Jari, Lindh Tuomo, Montonen Jan-Henri, Tikkanen Kyösti, Pyrhönen Olli Pekka

DOI: 10.1109/TIE.2019.2892665

Please cite the publication as follows:

Lana, A., Pinomaa, A., Peltoniemi, P., Lahtinen, J., Lindh, T., Montonen, J.-H., Tikkanen, K., Pyrhönen, O. P. (2019). Methodology of Power Distribution System Design for Hybrid Short Sea Shipping. IEEE Transactions on Industrial Electronics, vol. 66, issue 12. pp. 9591-9600. DOI: 10.1109/TIE.2019.2892665

Methodology of Power Distribution System Design for Hybrid Short Sea Shipping

***Abstract*—Application of energy storages (ES) in power distribution systems (PDS) of short sea shipping marine vessels is gaining ground. The main drivers are the increasing demand for higher energy efficiency and the decreasing costs of battery energy storage systems (BESS). The feasible chemistry and dimensioning of the BESS depend heavily on the vessel type, the PDS topology, and the load profile. Thus, no general rules for battery dimensioning that would fit all vessels can be presented, but the analysis must be performed by using an advanced modeling approach, which takes into account the above-mentioned factors. This paper presents a modeling methodology for dimensioning marine vessel ES and hybrid PDS components. The methodology has been tested for two distinct vessels, a cruiseferry and an off-shore support vessel (OSV).**

***Index Terms*—Hybridization, marine vessel, modeling.**

I. Introduction

HYBRIDIZATION of marine shipping vessels is gaining increasing attention. The main drivers are the growing demand for lower fuel consumption and emissions, higher energy efficiency, and decreasing costs of battery energy storage systems (BESS). The feasible battery chemistry and dimensioning of the storage system depend heavily on the vessel type, the PDS topology, and the load profile. Vessel hybridization has an effect on the capital and operational expenditures (CAPEX) and (OPEX), performance (improvement), and emissions (noise/vibration/pollution, and CO_2, NO_x, SO_x all reduced) of the vessel. In order to evaluate and quantify the above aspects by correct dimensioning of the hybrid PDS in the vessel operating profile, an approach for the techno-economic study of the marine vessel is required.

The present hybrid solutions are based on internal-combustion-engine-connected gensets, electrical power transmission, and electrical propulsion and thruster drives. The history, state of the art, and future trends in electric propulsion have been reviewed in [1], [2]. Owing to the fast development in battery technology [3], [4], there is an increasing interest in higher utilization of ESs specifically in short shipping hybrid solutions. Furthermore, the DNV GL maritime class society supports large maritime BESS [5]. A large-scale ES offers additional freedom to balance the electric energy production and consumption in any electric system. Batteries can increase the energy efficiency in vessel drive systems by taking over the fast power response responsibility from combustion engines and supporting the fast control actions of the vessel, where the stored energy can be used directly from the batteries. Additional benefits, such as energy savings and increased controllability and performance, can be achieved by combining new ES technologies with previous solutions.

With advances in secondary BES technologies, especially lithium-based chemistries [6], inclusion of high-energy or high-power battery packs in marine applications are becoming more attractive. An ES system can take on a wide range of functions [7], such as spinning reserve, enhanced ride through, peak shaving, enhanced dynamic performance, strategic loading, and zero emissions operation. The benefits of including ES in the electrical network of hybrid and full-electric ships are discussed in [8]. In [9], the benefits and drawbacks of installing batteries in OSVs have been investigated.

According to the literature, the costs of battery packs for EVs and utility-scale applications are decreasing [10], [11]. Furthermore, the same lithium cells are used in marine-rated battery packs, and could thus be expected to share the same trend of cost reduction. Other types of ESs for marine applications are fuel cells for long-term high energy application and ultracapacitors for short-term high-power applications; also flywheels have been considered for specific cases.

A review of current and future power and propulsion system architectures and their control strategies for smart ships is given in [12]; the authors emphasize that in order to determine the optimal architecture, knowledge of the operating profile is a prerequisite. High-level algorithms control the hybrid vessel power plant, power generation, propulsion drives, and battery usage in order to match the generation and loads during vessel operation. A genetic algorithm (GA) based approach can be used for the optimal scheduling of the diesel generators (DG) and to minimize the fuel consumption (FC) [13], [14]. The fuel consumption is analyzed for optimal load sharing among the DGs in the DC PDS architecture by applying a Particle Swarm Optimization (PSO) algorithm presented in [15]. Optimal scheduling is reported and discussed in [16], where the Harmony Search (HS) algorithm is used and compared with conventional algorithms and evolutionary algorithms MinMax, MinCon Methods as well as GA, PSO, and HS under both the scenarios of equal and unequal ratings of diesel generators.

The control of directly connected ES in diesel electric vessel drives and the related benefits have been studied in [17]. The ES makes it possible to reduce load variations of the diesel and the generator, leading to fuel savings, especially during the dynamic positioning (DP) mode of the OSV. A nonlinear programming method has been used to identify the optimal power sharing criteria between the generators and the ES, and a control strategy is presented in [18].

Vessel hybridization requires optimal dimensioning of the PDS components. A methodology to find the optimal size of a hybrid PDS is presented in [19], where an optimal sizing problem is formulated as a constrained nonlinear optimization problem, Multi-Objective PSO (MOPSO), combined with an elitist nondominated sorting genetic algorithm (NSGA-II), and used to solve the multi-objective optimization problem.

Trends for more efficient and versatile ships have increased the variety in hybrid propulsion and power supply architectures [12]. LVDC and LVAC architectures were analyzed in [20], [21] in terms of fuel consumption, weight, volume, emissions, and reliability. A hybrid OSV with LVDC PDS was investigated in [18] in terms of fuel saving. To further increase the vessel energy efficiency, energy management strategies (EMS) are developed. A multischeme EMS for maximizing the system efficiency, covering state-based EMS, equivalent fuel consumption minimization strategy (ECMS), charge-depleting charge-sustaining (CDCS) EMS, classical proportional-integral (PI) controller-based EMS, with performance comparisons for a hybrid vessel was presented in [22], [23]. The EMSs for ES devices and a DC grid were designed, tested, and verified in a laboratory and by using a simulator in [24]–[27]. EMS algorithms based on mixed-integer linear programming (MILP) were proposed as a strategy for optimal unit commitment in power generation in [28].

In this paper, methodology for the dimensioning of vessel ESs is presented and showcased by two vessels from different marine segment. The multilevel target is to define dimensioning rules for the BESS. The vessels under the hybridization study are a cruiseferry and an OSV. Thus, the ES dimensioning has to be carried out in the power range from hundreds of kW to several MW, for a PDS operating at medium- (MV) and low-voltage (LV) levels.

The aim of the proposed methodology is to obtain quantitative results on the specific fuel oil consumption (SFOC) of the vessel engines; to estimate the PDS efficiency and energy loss in the PDS components; to achieve an estimate of the ES load/capacity profile with the given EMS rules, including the peak power requirement for the grid interface components and the ES configuration, and the capacity requirement. Finally, the paper aims at estimating the ES Ah throughput and lifetime. Such estimates enable techno-economic evaluation of the OPEX and CAPEX of the hybrid vessel concept.

This paper is constructed as follows: The approaches for modeling and computational methodology are presented in Section II, and they are applied to the case vessels in Section III. Accuracy of the methodology is verified in Section IV. The main results and their significance for the research field are discussed in Section V.

II. Methodology

A. Modeling methodology

The developed methodology is based on original operating profile data of a nonhybrid vessel. The objective of the approach is to estimate the efficiency of the PDS, from fuel to propulsion power, and dimension the hybrid PDS components to allow operation according to the original operating profile.

The vessel operating profile and the power plant loading requirements should be known. The proposed methodology uses a data set with a second-level resolution because of the steady-state power-flow-based computation, where the dynamics and the transient behavior are not modeled. This allows fast computation and provides a means to analyze vessel operations of a long duration. The knowledge of individual engine loading, again, allows to use the original scheduling of engines in computation, and thus, corresponds to actual conditions and usage patterns. For the analysis of the vessel PDS and fuel efficiency, knowledge of the architecture and configuration of the power plant and the PDS, including the efficiency of the PDS and power plant components, is required. This enables analyses where advanced hybrid architectures can be proposed and developed for this type of a vessel and compared with original configurations in terms of fuel efficiency, losses, and PDS efficiency. The knowledge of the vessel size, capacity, and objectives related to the BESS operations provide the initial requirements for the BESS type and chemistry and also set the maximum boundaries on the volume and weight of the BESS. Further, the PDS interface components are configured according to the BESS type and its properties. The properties of the BESS include the round-trip efficiency (charging and discharging efficiencies) of the BESS chemistry, the discharge capability (the maximum current sourcing, peak and continuous), the storage capacity dependence on the discharge current, and the Ah throughput. The level and number of details required of the BESS depend on the targets and depth of the analysis.

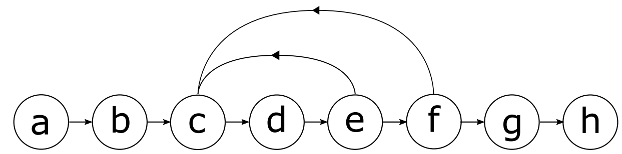

Fig. 1: Process sequence.

The process sequence of the proposed modeling method is illustrated in Fig. 1, and it comprises the following steps:

(a) Model the power plant, PDS configuration, the power flow, and the efficiency maps of the diesel engines, DGs, drives/interfacing power electronics and transformers, and the ES for the selected PDS architecture and voltage level.
(b) Identify the operating modes (OM) from the data set.
(c) Form the rules for each OM and scenario.
(d) Compute the hybrid operating profile.
(e) Check for the correspondence with the initial objectives, PDS and restrictions of the components; if needed, adjust the dimensions of the components or rules, go to step (c).
(f) Proceed with steps (c)–(e) for the available data and OM.
(g) Form annual results by combining daily route data or the data from different OMs with vessel annual distributions.
(h) Save the results for the vessel configuration.

B. Computation methodology

The results from the above sequence are not be based on optimum PDS dimensioning, neither an optimum EMS rule set. In this paper, the focus is on the design of a computation methodology that is performing outside the optimization algorithm as a black box model. The optimization problem statement for the given vessel operating profile (route, mode, power, load) is to determine the vessel PDS configuration, the engine (and BESS) schedule, and the EMS rules that minimize the investment payback time, where an optimal match between OPEX (fuel consumption, running hours, number of BESS cycles) and CAPEX (number of engines, PDS configuration) of the vessel is found. This is an MILP problem [28]. To find an optimum solution, dynamic programming algorithms, a Branch-and-bound algorithm, or a Mixed Integer Distributed Ant Colony Optimization (MIDACO) algorithm with a parallelization approach [29] could be applied. The methodology presented here could be applied by a combination with a optimization solver according to the following steps:

(a) Identify the operating modes from the load profile (application of time series identification and machine learning).
(b) Form the EMS rules.
(c) Define and set the objective function for each operating mode, for instance, minimize the fuel consumption.
(d) Define the decision variables, which are:
  - PDS architecture: traditional/BESS-enabled hybrid AC and DC PDS with full electric/hybrid propulsion.
  - PDS components: BESS capacity and power, nominal power and number of the diesel genset, and
  - EMS rule set.
(e) Define the constraints: max. capacity/power, allowed number of start/stops, cycle life, vessel operating constraints.
(f) Run the optimization solver.
(g) Form the annual results for the optimized solution.

The general computation flow is presented in Fig. 2. The input is the load profile of the DGs of a nonhybrid vessel and information of the vessel under investigation. With these, an estimate of the original propulsion load is obtained (block 1 in Fig. 2). The hybrid PDS configuration, EMS, and control systems are modeled with the aim of operating the vessel PDS according to the requirements and operating range of single components. The results of the computation are the data sets of hybrid power plant loads, control and energy management actions, and resulting fuel consumption. Based on the data sets, estimates of the energy and power requirements, the Ah throughput, the cycle life of the BESS, and the fuel consumption and the PDS efficiency are produced. In the computation, a simple moving average (SMA) is used (block 10 in Fig. 2). Measured data are used as the load forecast instead of estimates owing to the scheduled route of the vessel and the available weather forecast, and thereby, predictable load changes. An ideal prediction horizon could be parametrized and set according to the case vessel and the operating scenario. Also for the case of unpredicted changes in load, an SMA is calculated using only history records. In the next sections, the computation methodology is described:

1) Generator scheduling: In cases where generator scheduling is modified from the original vessel operation, the number of DGs in operation is set according to the power plant load using engine scheduling rules (logic-based EMS algorithms in block 2 shown in Fig. 2), such as Table I presents for the cruiseferry case. The output power of the engines is calculated from the power references and the nominal load and unload ramps of engines under consideration by the DG nominal ramping (block 3 in Fig. 2). The block is based on limiting the rate of change of the actual engine power output.

2) Power losses and PDS efficiency: In this section, computation of the PDS losses is described. The PDS losses

TABLE I: Logic for engine scheduling.

$P_{\mathrm{PDS}}^{\mathrm{MA1200}}$, pu $>$	$P_{\mathrm{PDS}}^{\mathrm{MA1200}}$, pu $<$	BESS SOC, %	DG RUNNING CONSTANT	DG RUNNING VARIABLE
0	1	>99	0	0
		>85	0	1
		40–85	1	2
		<40	1	2
1	2	>99	0	1
		>85	1	2
		40–85	1	2
		<40	2	2
2	3	>99	2	1
		>85	2	2
		40–85	2	2
		<40	3	2
3	4	>99	2	1
		>85	3	2
		40–85	3	2
		<40	3	2

and the power flow depend on the PDS architecture, configuration, and components. Black box modeling of the PDS component efficiencies and losses is used, and the components are described by single-point efficiency (could be weighted) or with an efficiency curve. A white or gray model of the electric components could also be used, as for instance in [14], [30], but it would require detailed data of the components and verification by measurements, and could result in unnecessary complexity of calculations, increasing the case processing time. However, if the objective of the analysis is set at the specific component or component parameter selection or sensitivity analysis, with the well-known properties and topology of the PDS components, detailed models could be included and used in the computation. In general, it can be stated for the system active power flow that

$$\begin{cases} P_{\mathrm{in}}^{\mathrm{pds}}(t) = \eta_{\mathrm{pe}}\eta_{\mathrm{G}}P_{\mathrm{out}}^{\mathrm{eng}}(t) \\ P_{\mathrm{out}}^{\mathrm{prop}}(t) = \eta_{\mathrm{tr}}\eta_{\mathrm{pe}}\eta_{\mathrm{M}}P_{\mathrm{out}}^{\mathrm{pds}}(t) \\ P_{\mathrm{in}}^{\mathrm{hotel}}(t) = \eta_{\mathrm{pe}}\eta_{\mathrm{tr}}P_{\mathrm{out}}^{\mathrm{pds}}(t) \\ P_{\mathrm{in}}^{\mathrm{ess}}(t) = \eta_{\mathrm{tr}}\eta_{\mathrm{pe}}\eta_{\mathrm{charging}}P_{\mathrm{out}}^{\mathrm{pds}}(t) \\ P_{\mathrm{in}}^{\mathrm{pds}}(t) = \eta_{\mathrm{tr}}\eta_{\mathrm{pe}}\eta_{\mathrm{discharging}}P_{\mathrm{out}}^{\mathrm{bess}}(t) \\ E^{\mathrm{ess}}(t) = \int_0^t (P_{\mathrm{in}}^{\mathrm{bess}}(t)dt - P_{\mathrm{out}}^{\mathrm{bess}}(t)dt) \\ P_{\mathrm{in}}^{\mathrm{pds}}(t) = P_{\mathrm{out}}^{\mathrm{pds}}(t), \end{cases} \tag{1}$$

where η_{pe} is the efficiency of the converter, η_{tr} is the efficiency of the transformer, η_{G} is the efficiency of the generator, η_{M} is the efficiency of the motor, and η_{charging} and $\eta_{\mathrm{discharging}}$ are the efficiencies of the battery charging and discharging. P with a different superscript is used to indicate the component power: engine (eng), BESS (bess), hotel load (hotel), propulsion motors (prop), network (pds), and the subscripts power intake (in), power outtake (out). The corresponding efficiencies are used in power loss blocks 4–6 and 9 (Fig. 2). The efficiencies of the PDS components used in this paper are acquired from publicly available sources given by component manufacturers. The voltage and power ratings of the components are set according

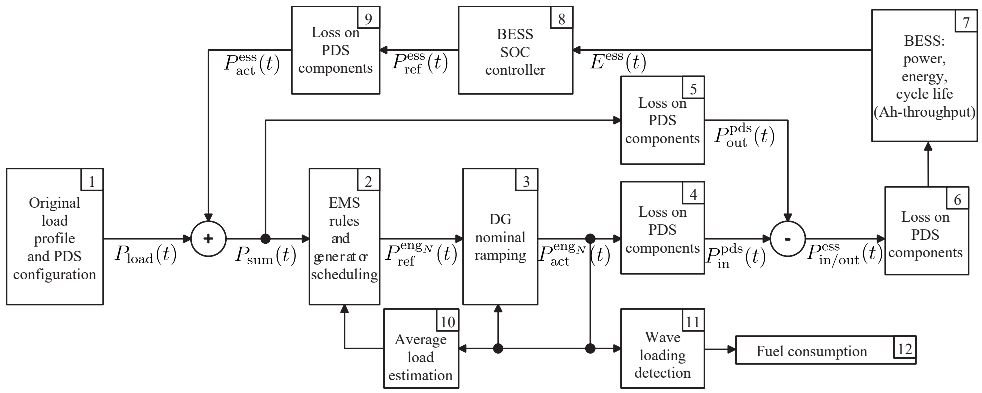

Fig. 2: Computation diagram.

TABLE II: Efficiencies of the PDS components.

Description	Stages	Efficiency, %
Transformers. Propulsion and BESS transformer (MV/LV), LV distribution transformer	MV/LV, LV/LV	99
Generator converter, with active rectifier unit	AC/DC	98.84
Generator converter, with diode rectifier unit	AC/DC	99.66
Propulsion frequency converter with 12-pulse diode rectifier (LSU)	AC/DC/AC	98
Propulsion frequency converter with 6-pulse IGCT/IGBT active rectifier unit (ARU),	AC/DC/AC	97.5
Propulsion motor drive	DC/AC	98.74
BESS converter	AC/DC	98.84
BESS converter	DC/DC	99
BESS converter (incl. LCL filter)	AC/DC/DC	97.46
Hotel load inverter (incl. LCL filter)	DC/AC	98.4
BESS round trip energy efficiency	-	96.04

to the PDS configuration and the power requirements of the case vessel; the PDS efficiencies used in the case studies are presented in Table II.

3) Fuel efficiency: The fuel consumption (block 12 in Fig. 2) of the vessel is

$$FC = \int_0^t \sum_{n=1}^{N} SFOC_n(P_n^{\text{eng}}(t)), \tag{2}$$

where $SFOC_n(P)$ is the fuel consumption map of the n-engine, and N is the number of engines.

4) Control of the BESS: The BESS is used to compensate the difference in the DG and the propulsion load. The control of the BESS state-of-charge (SoC) with a PI controller is presented in the diagram as the SoC controller (block 8 in Fig. 2) . The aim of the control is to maintain a sufficient capacity level to enable operation according to the operating rules. The parameters of the SoC controller are set according to the requirements set by the battery operating profile. Additionally, the energy level of the storage is taken into account in the engine scheduling; as Table I shows, in case of an overcharge, the number of engines in operation is reduced, whereas in case of insufficient charge the number is increased, thereby providing the necessary power or load for the ES.

5) Wave loading detection: The effect of the engine load dynamics on fuel consumption could be included in the computation. The wave loading detection (block 11 in Fig. 2) is a black box model, a measurement-based look-up table, where the parameters are the average load and the load fluctuation variance, and the output is the increase in the engine fuel consumption. If there are look-up table data available, the increase in fuel consumption could be set according to the load average and fluctuation range; therefore, the dynamics related to the engine fuel consumption will be included in the static model.

6) Life span of the BESS: The feasibility of the battery-based ES in a marine application depends significantly on the cost and life span of the battery pack. The types of aging are divided into calendar aging and cycle aging. In the modeling of calendar aging, the main variables are time and temperature, because the capacity fade and the resistance increase are mainly caused by thermal processes, which are linear with time [31]. In the modeling of cycle aging, the main factors considered are typically temperature, cycle number, ΔSoC, and voltage, while some studies also consider C-rate. In [32], the dependence of the capacity fade is $Ah^{0.55}$, where Ah is the cumulative charge delivered by the battery over its life. The capacity fade to 80% of the initial value is generally considered the end-of-life point for batteries. The lifetime data provided by manufacturers are based on well-defined test conditions. The lifetime of the battery is simply given as the time until the total Ah throughput is identical to the Ah throughput measured under certain constant conditions [33]. In the time-domain computation, the BESS complex load profile and the SoC are estimated. However, in the marine application, for safety and reliability reasons, the batteries are stored and used under a controlled environment in fixed conditions, and therefore, the main aging factor, temperature, is kept within a range specified by the manufacturer. For this reason and to reduce the complexity of the model, the lifetime expectations presented in case studies are calculated using a linear Ah throughput aging model (block 7 in Fig. 2) in the presented case studies, and the remaining cycle lifetime of the BESS is expressed as

$$RLT(t) = 2N_{\text{cycles}} 0.9 E_{\text{Ah}} - \int_0^t \frac{|P_{\text{bess}}(t)dt|}{V_{\text{bess}}(t)}, \tag{3}$$

where N_{cycles} is the nominal number of cycles (discharge and charge), E_{Ah} is the nominal capacity of the BESS, and $V_{\text{bess}}(t)$ is the battery pack DC voltage level. With such a simplified model, details related to the effect of the rate of charge/discharge, the depth of discharge, and the SoC level on the capacity fade are missing. However, as we deal with time-domain computations, more sophisticated approximations could also be used in this case.

III. Case study

The first vessel under study is a cruiseferry with a known daily route and a power plant with a nominal power around 30 MW. The vessel has a full electric propulsion system, four equal power gensets, and two propulsion units, and the architecture of the PDS is MVAC. The second case is an OSV with a known operating profile containing different OMs, the nominal power of the power plant being around 9 MW.

By using the developed methodology, the operating scenarios are examined in detail, and the fuel efficiency and the BESS lifetime are estimated for the AC and DC PDS architectures with hybrid and nonhybrid configurations. The scenario parameters and system configurations are presented by a quantitative comparison between the options. The hybrid vessel will probably not be operated exactly as the original one owing to the improved capabilities of the hybrid vessel and the objectives of optimal operation. Thus, the cases presented here do not intend to demonstrate optimal cases of hybrid vessel operation, but rather serve as examples of achieving different goals, dimensioning cases, and cases in which the comparison between the PDS concepts is made. In the case studies, the ES battery type is not an input parameter for the computation. Rather, a suitable type can be selected and configured based on the output of the computation and the requirements for the power and capacity of the BESS. The BESS lifetime is estimated in the case studies with the battery cell type based on the Li-ion nickel-manganese-cobalt (NMC) chemistry characteristics presented in Table III.

TABLE III: Battery storage characteristics.

Parameter	Value
Pack voltage, V	1000
Cell cycle life, cycles	8000
Charge/discharge capability (cont./peak)	3C/5C
Chemistry round-trip efficiency %	96
Calendar life, a	10

A. Cruiseferry

The operating scenarios of the cruiseferry are examined in detail, and the improvement in the fuel efficiency and the BESS lifetime is estimated for the MVAC and MVDC PDS topologies for the hybrid and traditional configurations. The hybrid MVDC and the hybrid MVAC cruiseferry vessel PDS configurations are presented in Fig. 3. No harbor charging of the BESS is considered in the presented cases, but in all cases the hotel loads are supplied from the harbor infrastructure for fair comparison. The efficiencies of the PDS components used in the computations are presented in Table II. In this case, the calculation is based on the load data of the vessel engines for 24 hours with one-second resolution. The vessel configuration includes four engines, and the load is allocated according to engine running hours and maintenance schedule, with up to three engines running in normal conditions.

1) Constant load and start/stop operation: A large ES, in theory, could allow operation in a single, best-efficiency set point of a diesel engine. The strategy goals are to keep the load of the DG sets in the most efficient point and maintain the BESS capacity. This strategy provides constant flat loading of the gensets (Fig. 4), but at the cost of a reduced lifetime of the BESS as a result of the high cycling of the ES (Fig. 5).

2) Stabilization: A small-capacity ES is only used to stabilize the load changes. The load is distributed according to the original cruiseferry operating profile. The BESS operation is based on an SMA window of 240 s (120 s history/forecast) for the DG references, nominal load/unload ramping is used for the DGs, and the control of the BESS SoC is implemented with a PI controller, with the reference set at the 70% SoC. The BESS operation is illustrated in Fig. 6.

3) Load leveling: In this case, a high-capacity BESS is used for load leveling. The strategy objectives are to keep the load of the DG sets within the highly efficient zone, to maximize the lowest load boundary, and to maintain the capacity of the BESS. In cases where rescheduling of engines is needed, the decision on the number of engines running is made based on the average load of the power plant load and the BESS capacity; this is illustrated in Table I, where $P_{\mathrm{PDS}}^{\mathrm{MA1200}}$ is the 1200 s power plant load average. A single action of change, connection/disconnection of the DG, is allowed in a 20 min window. The load is distributed equally to the running DGs. Hybrid power plant operation is illustrated in Fig. 7, and the BESS operation is illustrated in Fig. 8.

4) Cruiseferry case results obtained from the developed methodology are presented in Table IV, where CL is a constant load, LL denotes load leveling, and STAB refers to the stabilization strategy. For the stabilization strategy, a comparison between the PDS architectures is presented in Table V.

In a traditional cruiseferry vessel, the MVDC PDS architecture will allow DG variable speed operation and reduce the FC by 5% as a result of the increased efficiency of the engine when running at a variable speed. In hybrid vessels with a large BESS, DG constant power operation could be achieved, and the difference in fuel efficiency between MVDC and MVAC would be minimized by the operation of the ES. The hybrid vessel benefits are an up to 9% reduction in the FC for the MVDC PDS and an up to 6% reduction for the MVAC PDS, with a 10–36% reduction in the DG running hours. A hybrid vessel configuration with fewer engines than in the traditional solution could be feasible. With a smaller storage, in the stabilization scenario, most of the fuel savings are obtained by the variable speed operation of the DGs, whereas the effect of hybridization on the fuel savings is minor. In this case, the benefits of hybridization lie mainly in the extended lifetime of the engines and a decrease in the need for service.

B. OSV

The OSV is not operating on a constant daily route. Therefore, the operating profile should be analyzed in order to identify the modes in which the vessel is operating. Each

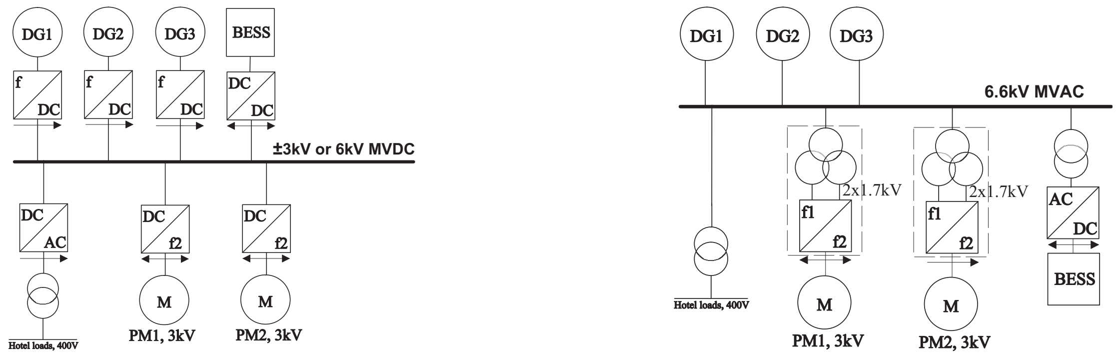

(a) (b)

Fig. 3: Simplified network topology of the cruiseferry vessel: (a) MVDC PDS, (b) MVAC PDS.

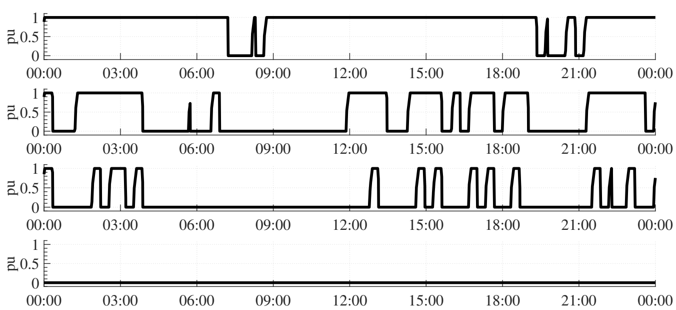

Fig. 4: Power plant operation in the constant load scenario.

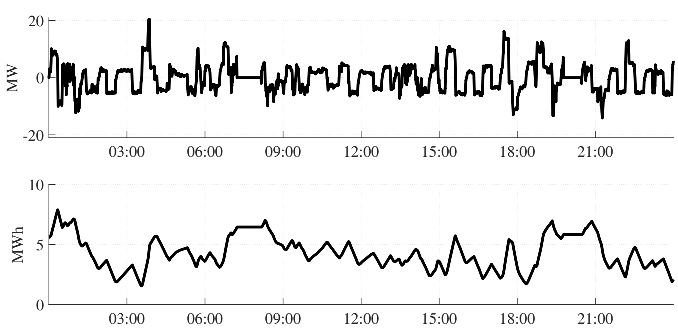

Fig. 5: BESS operation in the constant load scenario.

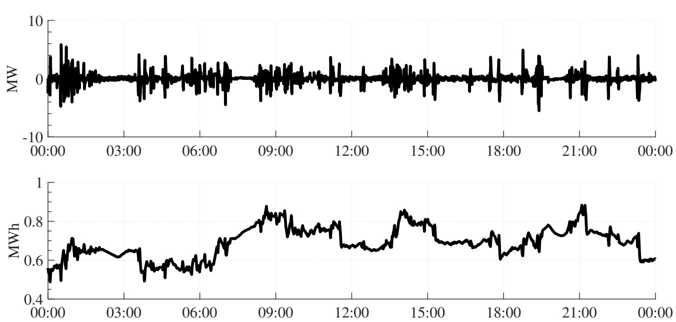

Fig. 6: BESS operation in the stabilization load scenario.

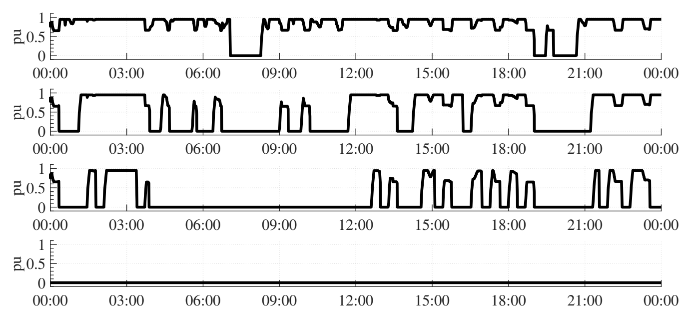

Fig. 7: Powerplant operation in the load leveling scenario.

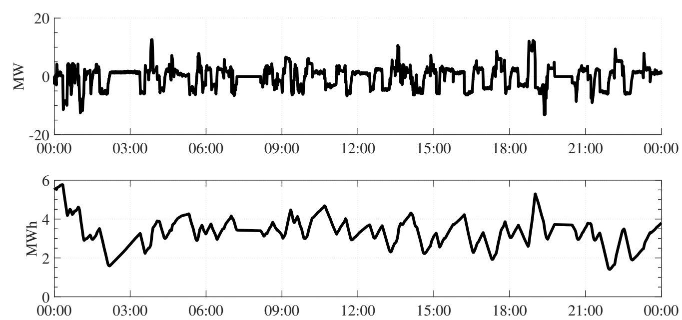

Fig. 8: BESS operation in the constant load leveling scenario.

TABLE IV: Comparison of the cruiseferry operation strategies.

Hybrid MVAC PDS, Operation strategy	**CL**	**LL**	**STAB**
Vessel FC reduction, %	5.78	5.5	0.32
DG running hours reduction, %	36	23	0
BESS Ah throughput, kAh/day	89	17	9.5
BESS lifetime estimate, a	1.8	6	6
BESS max. power , MW	20	8	5.8
BESS min. capacity, MWh	8	2	0.4

mode should be examined separately in order to establish a specific set of rules for the EMS of the hybrid vessel. For each operating mode, per hour result quantities are computed with the presented methodology and rescaled to annual results.

The annual distribution of the investigated OSV operating modes is presented in Table VI. A data set of two-week vessel operation was used as the input data. From the input data, different operating modes were identified. The investigated hybrid LVDC and hybrid LVAC configurations of the OSV PDS are presented in Fig. 9. The engine operating strategies for the case vessel are original scheduling, stabilization, and start/stop. In the stabilization strategy, the DG load reference

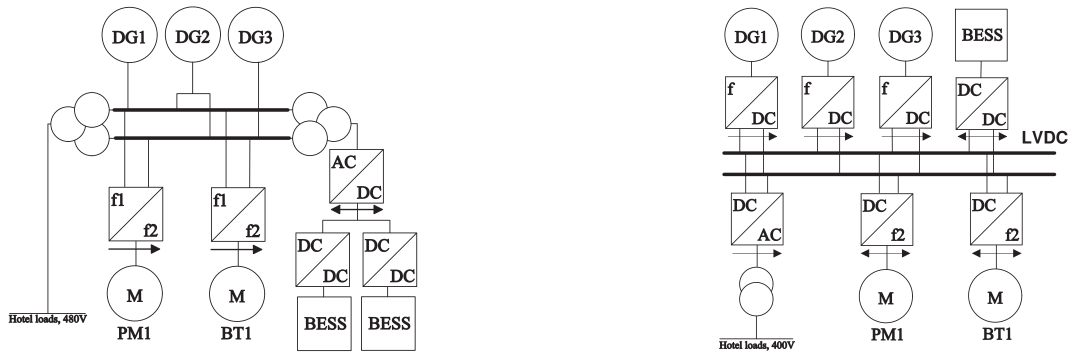

(a) (b)

Fig. 9: Simplified network topology of the offshore support vessel: (a) LVAC PDS, (b) LVDC PDS.

TABLE V: Comparison of the cruiseferry PDS configurations.

PDS architecture	Traditional		Hybrid	
	MVAC	MVDC	MVAC	MVDC
Vessel PDS EE, %	97.82	98.31	97.78	98.27
Vessel FC reduction, %	-	5.12	0.32	5.76
BESS Ah throughput, kAh/day	-	-	9.5	9.5
BESS lifetime estimate, a	-	-	6	6
BESS max. power, MW	-	-	5.8	5.8
BESS min. capacity, MWh	-	-	0.4	0.4

min. and max. are kept within the set boundaries to keep the engine running in the efficient range. Owing to the engine fuel consumption map differences for constant and variable speed engines, the DG load reference boundaries for the LVDC PDS are the minimum of 0.15 p.u. and the maximum of 0.85 p.u., and 0.15 p.u. and 1.0 p.u. for the LVAC PDS. In the start/stop strategy, the engines are running at a constant load in the best efficiency point. For the LVDC PDS, the DG load reference is constant at 0.85 p.u., and for the LVAC PDS at 1.0 p.u.

For the engine scheduling, the rules based on moving averages are used. An assumption that the energy management system can predict changes in the power plant load 10 min ahead is made. Therefore, actual measurement data are used as the forecast; results based on such an assumption are theoretical and indicate the potential when the load estimate is accurate. For the power plant load, a 10 min load forecast and 10 min history data with equal weighting for the long-term average and a 4 min average for the short-term average are used. For the BESS capacity, a 4 min history average is used. Out-of-order rescheduling is made on the following events: fast load change identification, with a 10 min and 4 min average comparison and power plant startup identification, based on a comparison between the load history and forecast.

The PDS efficiency calculations are based on data presented in Table II. A comparison of the start/stop and stabilization strategies for the OSV with the hybrid LVDC PDS running during the DP operations is presented in Table VII. Annual results for the different OSV PDSs are presented in Table VIII.

TABLE VI: Operating mode distribution for the OSV.

Operating mode	Annual, %	Speed, knots	Dataset, h
Transit high speed (THS)	4	14	26.2
Transit eco. speed heavy draft (TESHD)	2	12	26.2
Transit economical speed (TES)	12	12	46.3
Waiting on Weather (WOW)	4	0	46.3
Dynamic Positioning (DP)	39	0	62.8
Standby at Field (SBAF)	10	0	62.8
Alongside Quay (AQ)	29	0	119.4

TABLE VII: OSV operating strategies in the DP operations.

Hybrid LVDC PDS, Operation strategy	CL	STAB
PDS EE, %	94.2	97.4
Vessel FC reduction, %	48.6	37.8
DG running hours reduction, %	84	50
BESS Ah throughput, kAh / h	0.7	0.05
Number of start/stops	36	1
BESS max. power, MW	1.9	0.9
BESS min. capacity, MWh	0.3	0.1

TABLE VIII: Comparison of the OSV PDS configurations.

PDS architecture	Traditional		Hybrid	
	LVAC	LVDC	LVAC	LVDC
Vessel FC reduction, %	-	18.21	16.3	22
DG running hours reduction, %	-	-	41.6	40.7
BESS Ah throughput, kAh/a	-	-	392	485
BESS lifetime estimate, a	-	-	20	16
BESS max. power, MW	-	-	1.8	1.8
BESS min. capacity, kWh	-	-	180	155

IV. Verification of Methodology

A specific case of an OSV with an LVAC PDS operated in the DP mode is chosen to verify the accuracy of the presented methodology. The configurations under study are a two-genset configuration and a hybrid configuration with a single genset and an energy storage. The case vessel PDS is simulated in the Simulink environment with the dynamics of the power system and the power system control, and computed in the MATLAB with methodology proposed in the paper. The simulink model is based on average modeling [17], and it is computed with a time step of 5 µs and an ode45 solver. A real load profile of one-hour DP operation with one-second resolution of the OSV is used as an input to both models. A comparison of the simulated and computed results for the genset output power of the traditional LVAC PDS is presented in Fig. 10. Further, the comparison for the genset output power, and BESS load and capacity are presented in Fig. 11. The instantaneous genset power output differs between computations. In Simulink, the PDS losses are accurately predicted, and in the presented MATLAB computation, a single efficiency point of components is considered. The results on the FC and BESS Ah throughput are given in Table IX for the hybrid LVAC PDS.

Because the dynamics of the PDS is not presented in the steady-state computation, the load is distributed equally between the gensets (Fig. 10). Correspondingly, the constant load behavior does not indicate the genset and PDS interactions. Furthermore, the BESS response is instant and the dynamics of the BESS and PDS interactions is not included (Fig. 11). The results in Table IX verify the computation with the presented methodology and show the performance of the MATLAB steady-state computations. The Simulink model includes the PDS control and dynamics, which explains the difference in the results. As a result of the capacity requirement, it can be seen that the MATLAB model control over the BESS SoC differs from the Simulink model. For the selection and dimensioning of the vessel PDS components, the MATLAB-based computation produces results with one percent accuracy in comparison with the dynamic simulation. For such an accurate performance, information of the PDS configuration, components, and component efficiencies is needed. The same performance can be achieved in the energy management strategy evaluation. For instance, the OSV case evaluation with seven operating modes, six PDS configurations, and three EMS operating modes results in 126 cases and 2142 hours of data to be computed. This computation with the presented methodology including reporting of results by using MATLAB with a parallel pool on a modern workstation takes less than three hours.

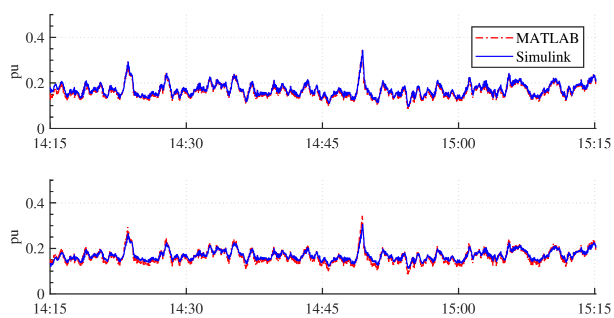

Fig. 10: Reference LVAC PDS genset 1 (upper) and 2 (lower) output power.

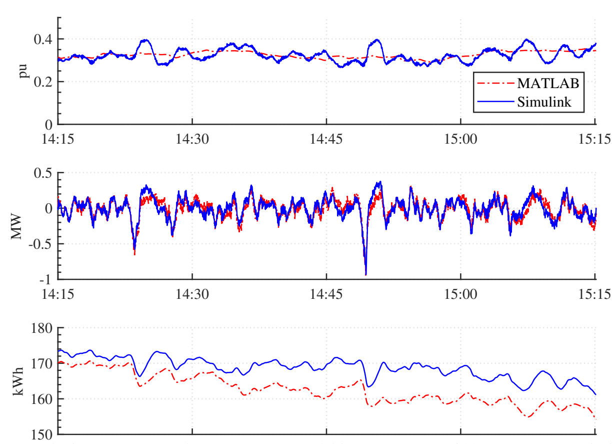

Fig. 11: Hybrid LVAC PDS genset output power and BESS power and capacity (from top to bottom).

TABLE IX: Comparison of the results of OSV DP operations.

Environment	**MATLAB**	**Simulink**	**Difference**
Model and computation nature	Steady	Dynamic	
Hybrid PDS fuel consumption, kg	176	175	1
BESS Ah-throughput, Ah	112	118	6
Vessel FC reduction, %	26	27	1
Req. BESS max. power, MW	0.93	0.95	0.02
Req. BESS min. capacity, kWh	17	13	4
Computation time	30 sec	8 hours	-

V. Discussion

The presented methodology enables computation of hybrid system dimensions and fuel efficiency without detailed information of the PDS components. The methodology allows trial of control concepts and an iterative approach, where the vessel operating profile, dimensioning of the engines, the ES capability, and the PDS topology and configuration are evaluated. Computation is implemented with MATLAB, and it can effectively utilize parallel pool computations. The energy management concepts developed with the presented methodology can be further enhanced by a detailed dynamic simulation of the PDS including control models in the Simulink Simscape Power Systems and verified by emulations in laboratory. Here, the uncertainties of the computations can be compensated for by close to real vessel measurements. The uncertainties in the methodology and computation originate for instance from the steady-state modeling, the DG fuel efficiency and transient loading model, the PE component efficiencies, the BESS transient response and aging model, and the control system. The presented methodology could be applied to any marine vessel with a known operating profile, power plant, and PDS configuration.

References

[1] E. Skjong, R. Volden, E. Rødskar, M. Molinas, T. A. Johansen, and J. Cunningham, "Past, present, and future challenges of the marine vessel's electrical power system," *IEEE Trans. Transport. Electrific.*, vol. 2, no. 4, pp. 522–537, Dec. 2016.

[2] J. F. Hansen and F. Wendt, "History and state of the art in commercial electric ship propulsion, integrated power systems, and future trends," *Proc. IEEE*, vol. 103, no. 12, pp. 2229–2242, Dec. 2015.
[3] E. Chemali, M. Preindl, P. Malysz, and A. Emadi, "Electrochemical and electrostatic energy storage and management systems for electric drive vehicles: State-of-the-art review and future trends," *Trans. Emerg. Sel. Topics Power Electron.*, vol. 4, no. 3, pp. 1117–1134, Sep. 2016.
[4] S. S. Williamson, A. K. Rathore, and F. Musavi, "Industrial electronics for electric transportation: Current state-of-the-art and future challenges," *IEEE Trans. Ind. Electron.*, vol. 62, no. 5, pp. 3021–3032, May. 2015.
[5] O. Alnes, S. Eriksen, and B. J. Vartdal, "Battery-powered ships: A class society perspective," *IEEE Electrific. Mag.*, vol. 5, no. 3, pp. 10–21, Sep. 2017.
[6] B. Scrosati and J. Garche, "Lithium batteries: Status, prospects and future," *J. Power Sources*, vol. 195, no. 9, pp. 2419 – 2430, 2010.
[7] J. O. Lindtjørn, F. Wendt, B. Gundersen, and J. Hansen, "Demonstrating the benefits of advanced power systems and energy storage for dp vessels," in *Proc. Dyn. Positioning Conf.*, pp. 1–23, 2014.
[8] G. S. Misyris, A. Marinopoulos, D. I. Doukas, T. Tengnér, and D. P. Labridis, "On battery state estimation algorithms for electric ship applications," *Electr. Power Syst. Res.*, vol. 151, pp. 115 – 124, 2017.
[9] H. E. Lindstad, G. S. Eskeland, and A. Rialland, "Batteries in offshore support vessels – pollution, climate impact and economics," *Transport. Research Part D: Transport and Environment*, vol. 50, pp. 409 – 417, 2017.
[10] B. Nykvist and M. Nilsson, "Rapidly falling costs of battery packs for electric vehicles," *Nature Climate Change*, vol. 5, no. 4, pp. 329–332, 2015.
[11] R. Kempener and E. Borden, "Battery storage for renewables: market status and technology outlook," *Int. Renewable Energy Agency (IRENA): Abu Dhabi, UAE*, 2015.
[12] R. Geertsma, R. Negenborn, K. Visser, and J. Hopman, "Design and control of hybrid power and propulsion systems for smart ships: A review of developments," *Appl. Energy*, vol. 194, no. Supplement C, pp. 30 – 54, 2017.
[13] S. Kamala, P. Chauhan, S. Panda, G. Wilson, X. Liu, and A. Gupta, "Optimal scheduling of diesel generators in offshore support vessels to minimize fuel consumption," in *Proc. of 41st Annual Conf. of the IEEE Ind. Electron (IECON)*, pp. 004 726–004 731, Nov. 2015.
[14] B. Zahedi, L. E. Norum, and K. B. Ludvigsen, "Optimized efficiency of all-electric ships by dc hybrid power systems," *J. Power Sources*, vol. 255, no. Supplement C, pp. 341 – 354, 2014.
[15] P. Chauhan, S. Kamala, S. Panda, G. Wilson, X. Liu, and A. Gupta, "Fuel efficiency improvement by optimal scheduling of diesel generators using pso in offshore support vessel with dc power system architecture," in *IEEE PES Asia-Pacific Power and Energy Eng. Conf. (APPEEC)*, pp. 1–6, Nov. 2015.
[16] P. Yadav, R. Kumar, S. Panda, and C. Chang, "An improved harmony search algorithm for optimal scheduling of the diesel generators in oil rig platforms," *Energy Convers. Manage.*, vol. 52, no. 2, pp. 893 – 902, 2011.
[17] A. Lana, K. Tikkanen, T. Lindh, and J. Partanen, "Control of directly connected energy storage in diesel electric vessel drives," in *Proc. of 15th IEEE Int. Power Electron. and Motion Contr. Conf. (PEMC)*, pp. DS1e.7–1–DS1e.7–6, Sep. 2012.
[18] O. C. Nebb, B. Zahedi, J. O. Lindtjorn, and L. Norum, "Increased fuel efficiency in ship lvdc power distribution systems," in *Proc. IEEE Vehicle Power Propul. Conf.*, pp. 564–568, Oct. 2012.
[19] H. Lan, S. Wen, Y.-Y. Hong, D. C. Yu, and L. Zhang, "Optimal sizing of hybrid pv/diesel/battery in ship power system," *Appl. Energy*, vol. 158, no. Supplement C, pp. 26 – 34, 2015.
[20] S. Kamala, P. Chauhan, S. Panda, G. Wilson, X. Liu, and A. Gupta, "An exercise to qualify lvac and lvdc power system architectures for a platform supply vessel," in *IEEE Transport. Electrific. Conf., Asia-Pacific (ITEC Asia-Pacific)*, pp. 332–337, Jun. 2016.
[21] S. Kamala, P. Chauhan, S. Panda, G. Wilson, X. Liu, and A. Gupta, "A methodology to qualify marine electrical propulsion system architectures for platform supply vessels," *IET Electr. Syst. in Transport.*, Dec. 2017.
[22] A. M. Bassam, A. B. Phillips, S. R. Turnock, and P. A. Wilson, "Development of a multi-scheme energy management strategy for a hybrid fuel cell driven passenger ship," *Int. J. Hydrogen Energy*, vol. 42, no. 1, pp. 623 – 635, 2017.
[23] J. Han, J.-F. Charpentier, and T. Tang, "An energy management system of a fuel cell/battery hybrid boat," *Energies*, vol. 7, no. 5, pp. 2799–2820, 2014.
[24] A. J. Sorensen *et al.*, "Toward safer, smarter, and greener ships: Using hybrid marine power plants," *IEEE Electrific. Mag.*, vol. 5, no. 3, pp. 68–73, Sep. 2017.
[25] M. R. Miyazaki, A. J. Sørensen, and B. J. Vartdal, "Hybrid marine power plants model validation with strategic loading," *IFAC-PapersOnLine*, vol. 49, no. 23, pp. 400 – 407, 2016.
[26] M. R. Miyazaki, A. J. Sørensen, N. Lefebvre, K. K. Yum, and E. Pedersen, "Hybrid modeling of strategic loading of a marine hybrid power plant with experimental validation," *IEEE Access*, vol. 4, pp. 8793–8804, 2016.
[27] M. R. Miyazaki, A. J. Sørensen, and B. J. Vartdal, "Reduction of fuel consumption on hybrid marine power plants by strategic loading with energy storage devices," *IEEE Power Energy Technol. Syst. J.*, vol. 3, no. 4, pp. 207–217, Dec. 2016.
[28] E. Skjong, T. A. Johansen, M. Molinas, and A. J. Sørensen, "Approaches to economic energy management in diesel-electric marine vessels," *IEEE Trans. on Transport. Electrific.*, vol. 3, no. 1, pp. 22–35, Mar. 2017.
[29] M. Schlueter and M. Munetomo, "Numerical assessment of the parallelization scalability on 200 minlp benchmarks," in *IEEE Congr. on Evol. Comput. (CEC)*, pp. 830–837, Jul. 2016.
[30] A. Lana *et al.*, "On low-voltage dc network customer-end inverter energy efficiency," *IEEE Trans. Smart Grid*, vol. 5, no. 6, pp. 2709–2717, Nov. 2014.
[31] A. Barré, B. Deguilhem, S. Grolleau, M. Gérard, F. Suard, and D. Riu, "A review on lithium-ion battery ageing mechanisms and estimations for automotive applications," *J. Power Sources*, vol. 241, pp. 680 – 689, 2013.
[32] J. Wang *et al.*, "Cycle-life model for graphite-lifepo4 cells," *J. Power Sources*, vol. 196, no. 8, pp. 3942 – 3948, 2011.
[33] D. U. Sauer and H. Wenzl, "Comparison of different approaches for lifetime prediction of electrochemical systems—using lead-acid batteries as example," *J. Power Sources*, vol. 176, no. 2, pp. 534 – 546, 2008.